Scholars Journal of Applied Medical Sciences
Abbreviated Key Title: Sch J App Med Sci
ISSN 2347-954X (Print) | ISSN 2320-6691 (Online)
Journal homepage: https://saspublishers.com

OPEN ACCESS

Human Anatomy

Hemolymph Nodes and Cancer: A Retrospective Histopathological Study of Digestive Tract and Breast Cancers in 20 Patients

Fei Zhen, MD, MS[2], Wei-Ren Pan, MD, PhD[1]*, Zhi-An Liu, MD, MS, PhD[1], Ya-Ning Zhu, MD, MS[3], Chuan-Xiang Ma, BBSci, MS[1], Yao Li, MD, MS[1], Fan-Qiang Zeng, MDip, MD[1]

[1]Department of Human Anatomy, College of Biomedical Sciences, Xuzhou Medical University, Xuzhou, Jiangsu, China
[2]Department of Pathology, Fengfeng General Hospital, North China Medical & Health Group, Handan, Hebei, China
[3]Department of Pathology, Huaian First People's Hospital, Huaian, Jiangsu, China

DOI: https://doi.org/10.36347/sjams.2026.v14i11.005 | **Received:** 11.09.2026 | **Accepted:** 03.11.2026 | **Published:** 07.11.2026

***Corresponding author:** Wei-Ren Pan, MD, PhD
Department of Human Anatomy, College of Biomedical Sciences, Xuzhou Medical University, Xuzhou, Jiangsu, China

Abstract | **Original Research Article**

Background: There is still a controversy about the existence and nature of HLN in the human body since Gibbes found some structures forming lymph nodes with blood in sinuses instead of the lymph between the renal artery and vein in three human subjects in 1884. ***Methods:*** A total of 412 paraffin blocks of peritumoral lymph nodes were retrieved from 20 patients who had been surgically treated for digestive tract and breast cancers from June 1, 2021, to February 6, 2022. Histological sections were mounted on slides, hematoxylin and eosin staining was performed as a routine procedure, and immunohistochemical staining was performed using enzyme-linked immunosorbent assay kits. All slides were scanned using a slide scanner and observed using CaseViewer software. Twenty slides were observed using a confocal laser scanning microscope with a Leica Application Suite X. All data were collected and analyzed. ***Results:*** After 412 slides were observed, 334 were non-metastatic and 78 were metastatic. The phenomenon with characteristics of HLN was found in both non-metastatic (197 out of 334) and metastatic (18 out of 78) lymph nodes. Four pathological or histological types were identified based on the distribution characteristics of erythrocytes, macrophageerythrocyte-lymphocyte (MEL), and macrophage-lymphocyte (ML) rosettes in the dilated sinuses of the nodes. The detailed cellular features of the MEL and ML rosettes were determined. Binuclear macrophages, as well as binuclear, trinuclear, and tetranuclear lymphocytes, were detected in some lymph nodes. ***Conclusion:*** HLN were found in the peritumoral tissue of 20 cancer patients. The various histopathological and cytological changes of HLN were static manifestations of dynamic regeneration process of the degenerating lymph node in tumor immunity.

Keywords: Hemolymph node; erythrocyte; macrophage-erythrocyte-lymphocyte rosette; macrophage-lymphocyte rosette; digestive tract cancer; breast cancer.

Copyright © 2026 The Author(s): This is an open-access article distributed under the terms of the Creative Commons Attribution **4.0 International License (CC BY-NC 4.0)** which permits unrestricted use, distribution, and reproduction in any medium for non-commercial use provided the original author and source are credited.

INTRODUCTION

In 1884, Gibbes found some brownish-red structures between the renal artery and vein in three human participants, which resembled blood rather than the lymph in sinuses [1]. Subsequently, Robertson (1890) stated that these structures could be found in both human and animal subjects [2]. Consequently, he named them "Hemolymph node" (HLN). Thereafter, studies have shown that these nodes were mainly distributed around the kidneys, spleen, mesentery, thymus, and large arteries. It was considered that the node possessed afferent and efferent lymphatic vessels, and contained both blood and lymph [3-11]. These studies focused mainly on the morphological distribution and structure of the HLN, or the origin and location of erythrocytes in the sinuses, and seldom on the phenomenon of macrophage-erythrocyte rosette formation. However, an isolated report mentioned that the appearance of HLN might be related to immunoreaction of the body [12], but there was no strong evidence to support this view. Moreover, whether HLN was observed in the human body has been controversial [10, 13]. Recently, a rat HLN model was established by transferring allogeneic renal tissue [14]. Additionally, the rat HLN model could also be established by injecting allogeneic cancer cells and *Escherichia coli*.

Furthermore, details of the distribution and morphology of the HLN were revealed. Abundant erythrocytes and rosettes formed by MEL and ML were found in the sinuses of HLN within 7 days after allogeneic renal tissue transfer. Notably, rosettes were

found to be the key cellular complexes involved in the immune response.

In this study, peritumoral lymph nodes of the digestive tract and breast cancers in 20 patients were studied to clarify the histopathological structure of HLN and the cellular features of MEL and ML rosettes. The characteristic changes of macrophages and lymphocytes in the nodes that determine the presence of HLN was a manifestation of the immune reaction. As each lymph node was embedded in paraffin, the appearance of lymph nodes could not be observed macroscopically; therefore, the criteria for evaluating HLN was based on the microscopic findings of a previous study [14].

Materials and Methods

This study was performed with appropriate institutional ethics approval (approval no.: KY2022-110-01) in accordance with the principles of the Declaration of Helsinki.

A total of 412 paraffin blocks of lymph nodes were retrieved from the Department of Pathology of Huaian First People's Hospital, Huaian, Jiangsu, China. These nodes were harvested and pathologically diagnosed from peritumoral tissues of specimens obtained from 20 patients (14 males and 6 females, age between 50 and 81 years-old, average 66.45 years) with gastrointestinal or breast cancer who underwent surgical treatment between June 1, 2021, and February 6, 2022. All enrolled specimens finished the study, there was no attrition.

For all paraffin blocks, histological sections were mounted on glass slides (Leica RM2235, Leica Biosystems Trading Co. Ltd., Shanghai, China) and hematoxylin-eosin (HE) (Dako Coverstainer, Agilent CrossLab, Beijing, China) staining were performed using a routine procedure. Immunohistochemistry (IHC) was performed using ELISA kits (LYVE-1, CD3, CD5, CD19, CD68, CD79, and CD138, Zhongshan Jinqiao Biotechnology Co., Ltd., Beijing, China) via immunohistochemical staining (PT200, Agilent CrossLab, Beijing, China). All slides were scanned using a slide scanner (Pannoramic Scan; 3DHISTECH Ltd., Budapest, Hungary) and observed using CaseViewer software (CaseViewer; 3DHISTECH Ltd.). Twenty slides were observed, and images were captured using a confocal laser scanning microscope (Leica STELLARIS 5, Microsystems Trading Co. Ltd., Germany) with Leica Application Suite X software (LAS X; Leica Microsystems Trading Co. Ltd., Germany). All data were collected and analyzed.

The criteria for evaluating HLN were based on microscopic findings from a previous study (Pan *et al.,* 2023), whether they were filled with numerous erythrocytes, MEL, and ML rosettes in the sinuses of the node.

Results

Overview

A total of 412 lymph node slides were observed, 334 of which were non-metastatic nodes and 78 were metastatic (Table 1; Fig. 1). They were circular, oval, or polygonal in shape. The largest was 29 mm, and the smallest was 1 mm (average 5.5 mm) in length. A large number of erythrocytes and MEL rosettes were observed in the dilated sinuses of both non-metastatic (197 of 334 nodes) and metastatic (18 of 78 nodes) lymph nodes (Table 1; Fig. 1). In some sections, ML rosettes were present in the dilated sinuses of the nodes.

Table 1: Overall distribution of the peritumoral, metastatic, non-metastatic nodes, and HLN in patients

Specimen No	Sex	Age	Disease	MLN/TLN	HLN/NLN	HLN/MLN
1. 21-15149	M	60	Colon Ca.(R)	0/20	11/20	0/0
2. 21-15150	M	76	Cardiac Ca.	1/22	9/ 21	0/1
3. 21-15151	M	64	Cardiac Ca.	0/17	11/17	0/0
4. 21-15712	F	73	Esophageal Ca.	18/19	1/1	2/18
5. 21-18021	F	81	Gastric & colonic Ca.(R)	1/40	16/39	1/1
6. 21-18747	M	64	Rectal Ca.	0/12.	8/12	0/0
7. 21-19425	M	66	Esophageal Ca.	0/17	5/17	0/0
8. 21-20247	F	74	Breast Ca. (R)	8/14	3/6	5/8
9. 21-20783	F	71	Cardiac Ca.	0/33	11/33	0/0
10. 21-23217	M	66	Gastric Ca.	13/33	12/20	2/13
11. 21-23475	M	74	Cardiac Ca.	7/25	17/18	1/7
12. 21-23611	M	72	Cardiac Ca.	3/31	24/28	1/3
13. 21-28566	M	70	Esophageal Ca.	0/11	7/11	0/0
14. 21-30038	M	57	Sigmoid Ca.	0/13	11/13	0/0
15. 21-30396	M	58	Esophageal Ca.	3/20	7/17	0/3
16. 21-30877	F	56	Breast Ca. (R)	13/19	4/6	4/13
17. 21-31780	M	50	Rectal Ca.	3/9	4/6	0/3
18. 22-1442	M	76	Gastric Ca.	7/17	9/10	4/7

19. 22-1444	M	56	Rectal Ca.	0/14	12/14	0/0
20. 22-2428	F	65	Esophageal Ca.	1/26	16/25	1/1
			Total	78/412	197/334	18/78

TLN, Total peritumoral node; MLN, Metastatic node; NLN, Non-metastatic node; HLN, Hemolymph node.

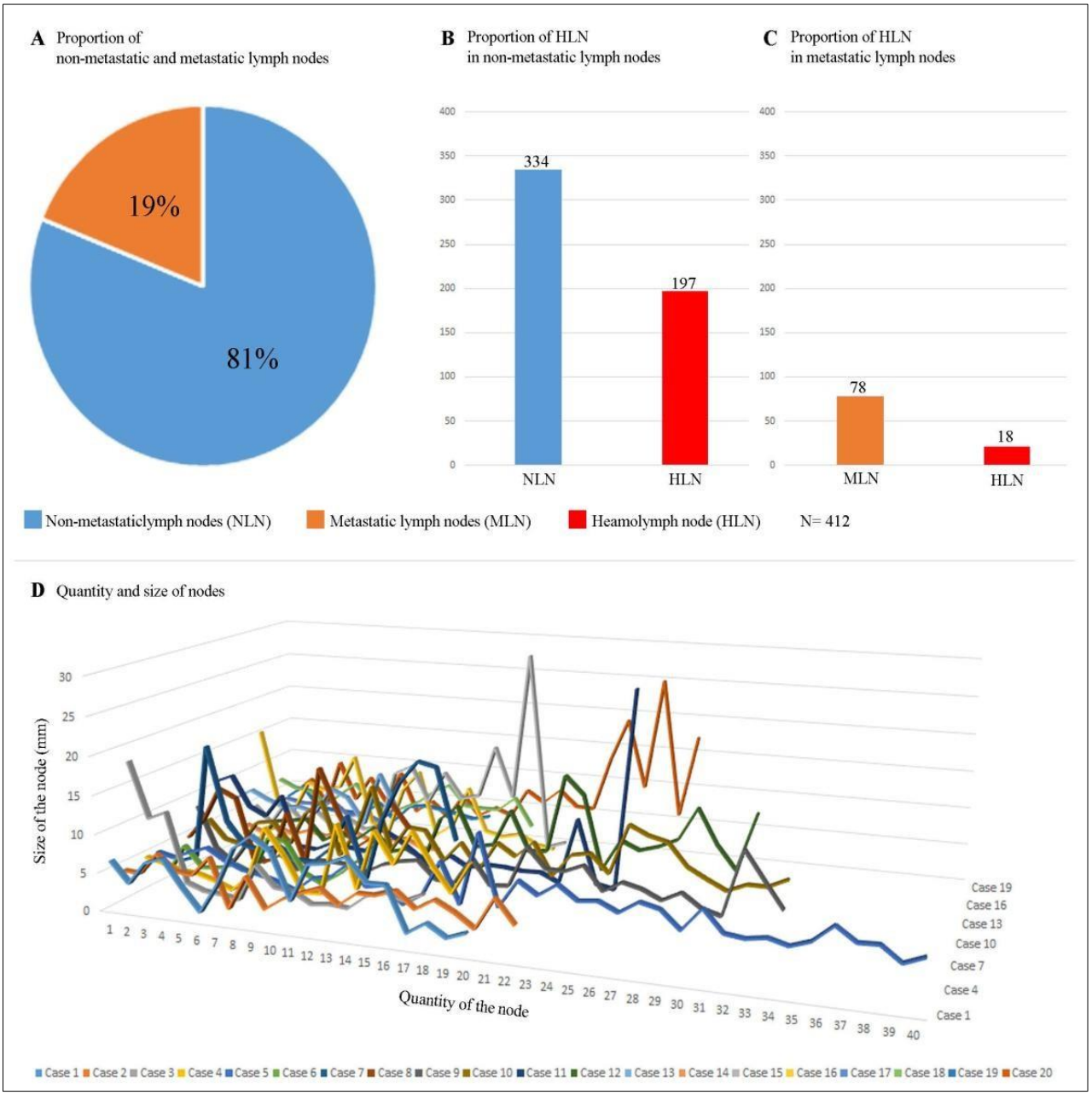


Figure 1. A to C: Statistical outcomes of peritumoral, metastatic, non-metastatic and hemolymph nodes in patients. D: Quantity and size of nodes

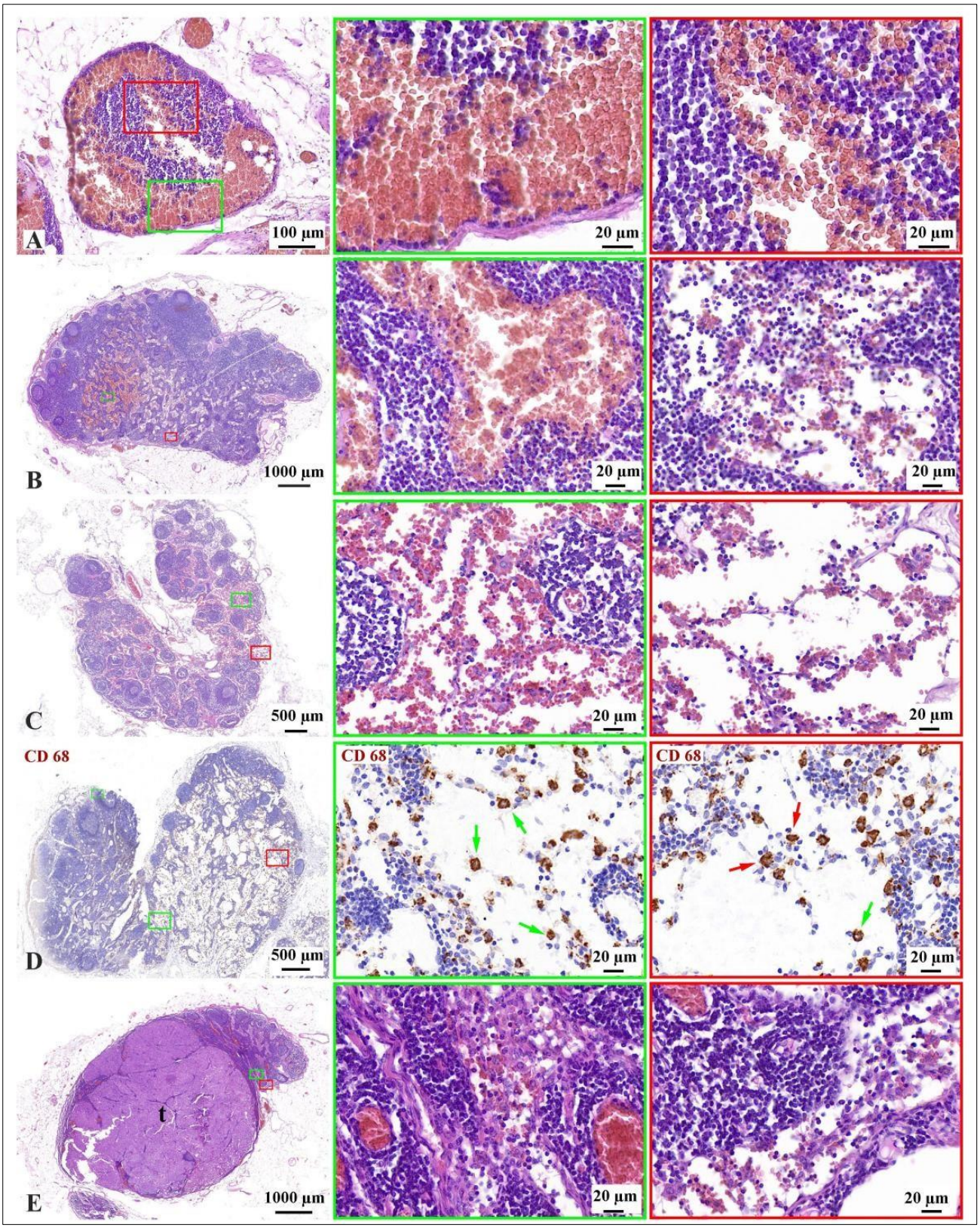


Figure 2: Histological type of HLN. The middle and right columns show magnified images of the green and red rectangular areas in the left column, respectively. (A) row: Histopathological type I HLN (HE). (B) row: Histopathlogical type II HLN (HE). (C) row: Histopathlogical type III HLN (HE). (D) row: Histopathological type IV HLN (CD68 IHC staining), MEL rosettes (green arrows), and ML rosettes (red arrows). (E) row: Metastatic lymph nodes with MEL rosettes in sinuses

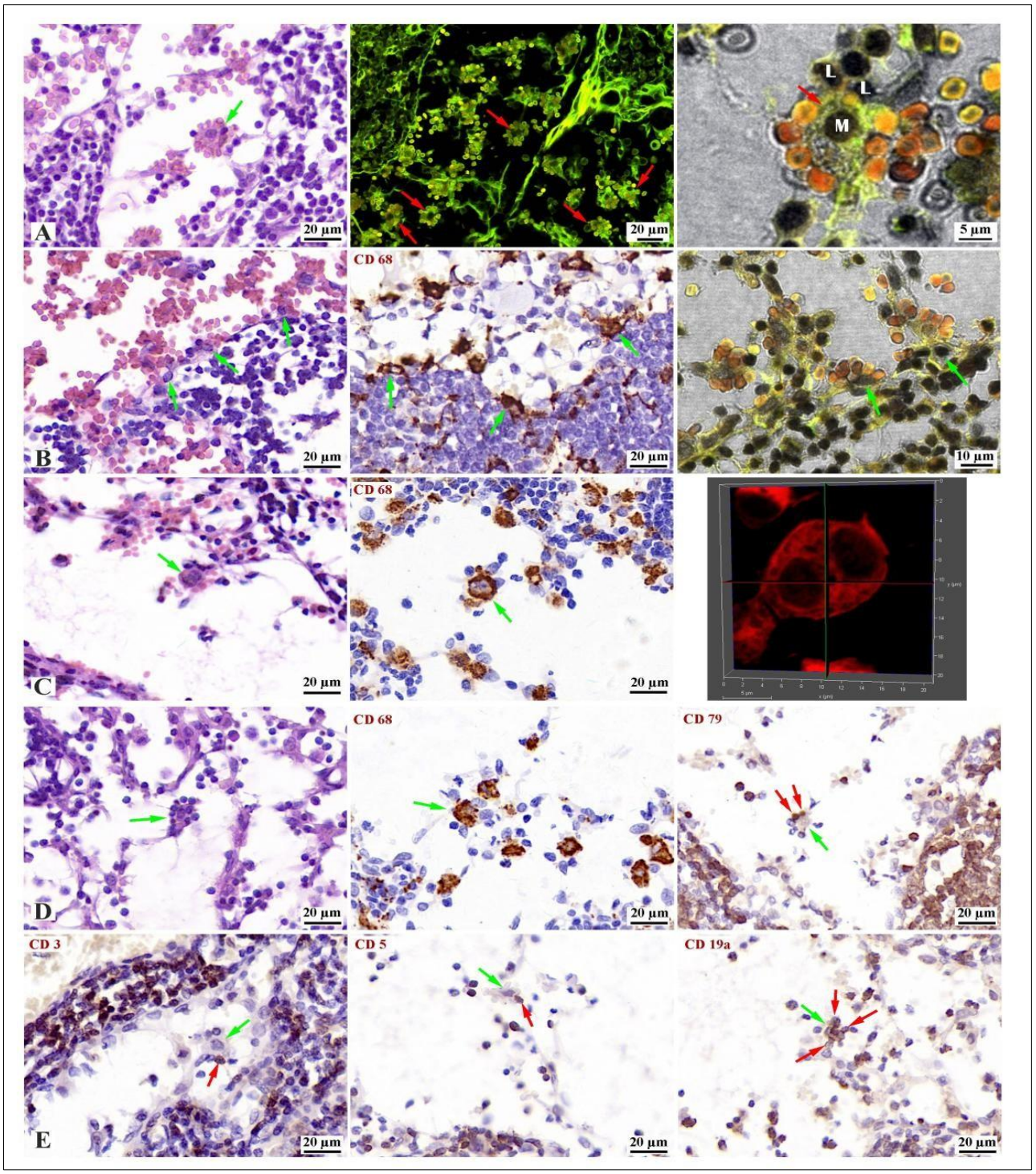


Figure 3. (A) row: The cellular structure of the MEL in the sinus is indicated by the green arrow in the left image (HE) and red arrows in the middle and right images (Confocal Laser Microscope Scanning [CLMS]), M = macrophages, L = lymphocytes. (B) row: MEL rosettes, those close to or partially passed through the sinus wall, have no RBC attachment on the side of the macrophage facing the parenchyma, indicated by green arrows in the left image (HE), middle image (IHC, CD68), and right image (CLMS). (C) row: Binuclear macrophages (promonocytes) adhered by erythrocytes in the dilated sinus (left image [HE], middle image [CD68], right image [CLMS]). (D) row: The cellular structure of ML in the sinus, indicated by green arrows in the left image (HE), middle image (CD68), and right image (CD79). Note: Two lymphocytes in the ML rosettes are stained by CD79 (red arrows). (E) row: The cellular structure of the ML in the sinus, indicated by green arrows. One lymphocyte of the ML rosette is stained by CD3 (red arrow in the left image), one lymphocyte of the rosette is stained by CD5 (red arrow in the middle image), and three lymphocytes of the rosettes are stained by CD19a (red arrows in the right image).

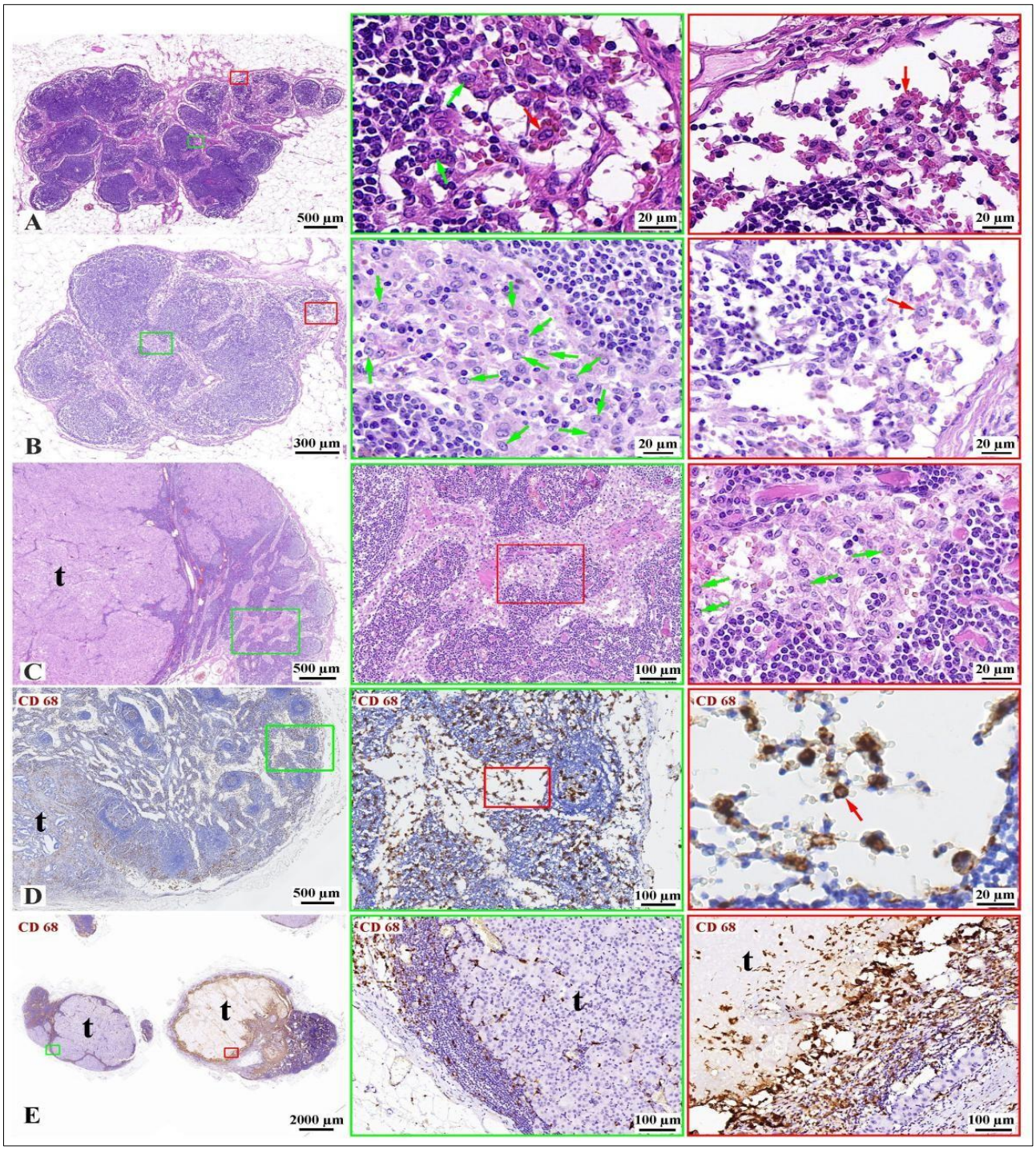


Figure 4. (A) row: The middle and right images are magnified images of the green and red rectangular areas in the left image (HE), respectively. The cellular structures of binuclear macrophages (promonocytes) (red arrow) and binuclear lymphocytes (green arrows) are indicated in the middle image. The MEL rosette is still present in the subcapsular sinus, indicated by the red arrow in the right image. (B) row: The middle and right images are magnified images of the green and red rectangular areas in the left figure (HE). Bi-, tri-, and tetra-nuclear lymphocytes are shown in the middle image (green arrows). The binuclear macrophage (promonocyte) adhered by erythrocytes is present in the dilated sinus of the node (red arrow). (C) row: A metastatic node (t = tumor). The middle figure is a magnified image of the green rectangular area in the left figure (HE). The right figure is a magnified image of the red rectangular area in the middle figure showing the bi-, tri-, and tetra-nuclear lymphocytes in the sinus of the node (green arrows). (D) row: A metastatic node (t). The middle figure is a magnified image of the green rectangular area in the left figure (CD68 stain). The right figure is a magnified image of the red rectangular area in the middle figure showing the binuclear macrophage (promonocyte) in the sinus of the node (red arrow). (E) row: Two metastatic lymph nodes are stained by CD68 in the left image. The middle and right figures are magnified images of the green and red rectangular areas in the left figure. The node on the right has a higher number of CD68(+) cells (macrophages) within and around the metastatic tumor and in the sinuses of the residual lymphoid tissue than the node in the middle image. The cellular structure of tumor cells (t) cannot be detected in the right image.

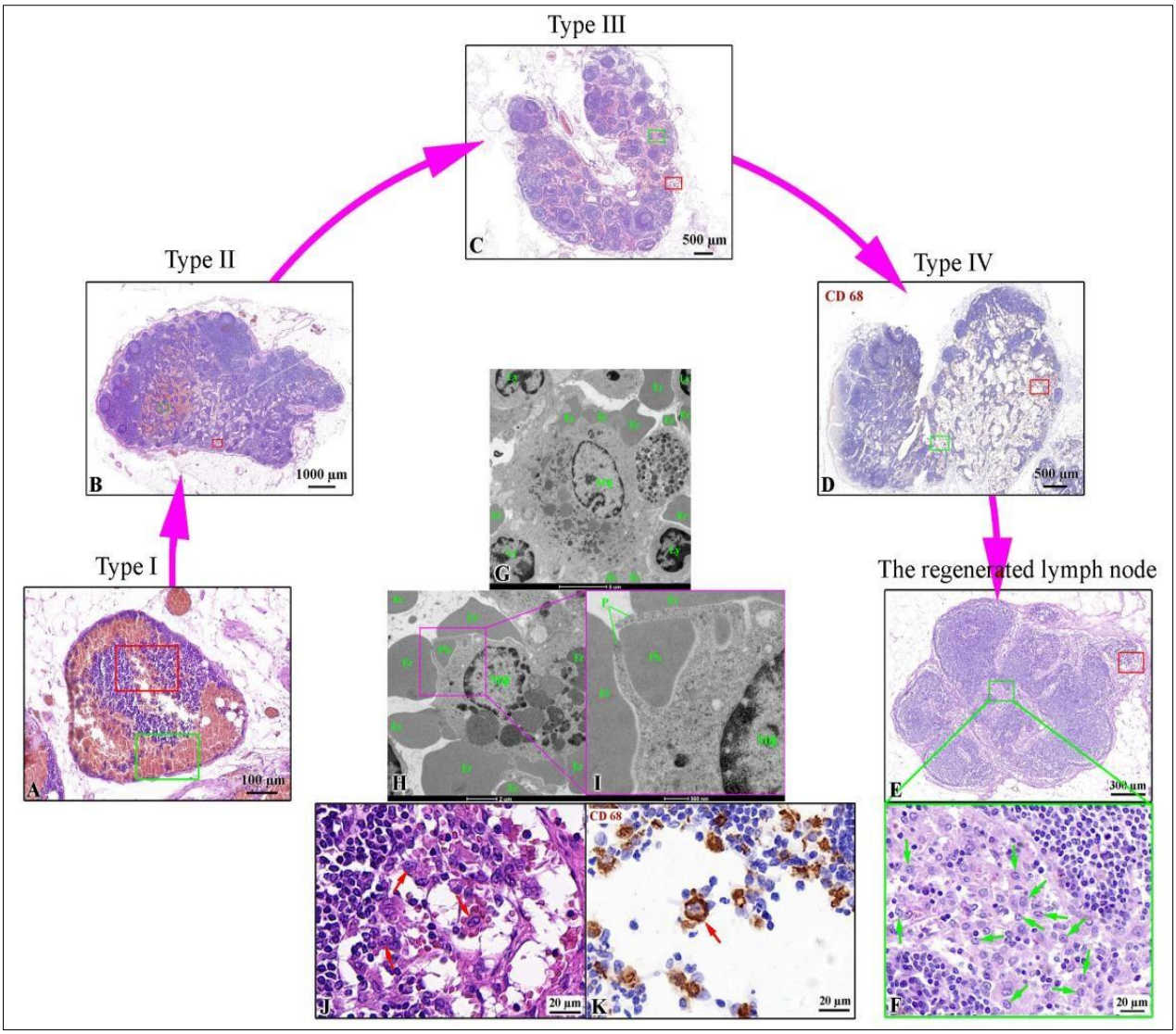


Figure 5: Static manifestations during the dynamic regeneration process of degenerated lymph nodes. A-D: Types of HLN. E-F: The regenerated lymph node. The lightly stained area (in image E) used to be dilated sinuses of the degenerated lymph node, but now it is filled with mono-, bi-, tri-, and tetra-nuclear (proliferating) lymphocytes (indicated by green arrows in image F). G-I: Transmission Electron Microscopic images of MEL rosettes. A MEL rosette contains a macrophage (Mϕ) surrounded by many erythrocytes (Er) and several lymphocytes (Ly). The macrophage extends its pseudopodia (P) to engulf a portion of the erythrocyte that becomes the phagosome. Macrophages contain many phagosomes used for cell proliferation (in images of G and H). J-K: Proliferating (bi- nuclear) macrophages (indicated by red arrows) in sinuses of the node.

Histopathological findings

Based on the histopathological and cellular features of the nodes, four types were identified:

Type I: Dilated sinuses were tightly packed with erythrocytes that mostly remained discoid shape (Fig. 2A row).

Type II: Some dilated sinuses were tightly packed with erythrocytes, whereas others were filled with MEL rosettes and scattered erythrocytes, some of which were irregularly shaped (Fig. 2B row).

Type III: Some dilated sinuses were filled with MEL rosettes surrounded by scattered erythrocytes, some of which were irregularly shaped (Fig. 2C row).

Type IV: Dilated sinuses were filled with either MEL or ML rosettes (Fig. 2D row).

Cytological findings

Each MEL rosette was composed of a macrophage in the center surrounded by numerous adherent erythrocytes, often one or two lymphocytes (Figs. 2 and 3A row). MEL rosettes, which were close to or partially passed through the sinus wall, had no RBC attachment to the side of the macrophages facing the parenchyma (Fig. 3B row). Microphages stained with CD68 were observed in both sinuses and parenchyma (Figs. 2D row, 3B middle image, and 3C middle image).

Each ML rosette was composed of a macrophage in the center adhered by 3 or more lymphocytes (Figs. 2D right image, 3C middle image, and 3D row). In addition, each lymphocyte adhered to a macrophage in a ML rosette was labeled by IHC staining, which indicated the subtype of the lymphocyte (Figs. 3D right image and 3E row). In some sections, the binuclear macrophage (promonocytes) was adhered by erythrocytes around (Figs. 3C, 4A, and 4B rows). Bi-, tri-, and tetra-nuclear lymphocytes (dividing lymphoblasts) (Figs. 4A and 4B rows) gathered in the dilated sinuses of the nodes.

This phenomenon was also observed in the sinuses of the residual lymphoid tissue in 18 of the 78 metastatic lymph nodes (Table 1; Figs. 1, 2E, 4C, and 4D rows). In 33 metastatic lymph nodes, a large number of CD68(+) cells (macrophages) were observed around and within the metastatic tumor, as well as in the sinuses of the residual lymphoid tissue in the node (Fig. 4E row). Cellular structures could not be observed within the tumor cells in two cases (Fig. 4D right image).

DISCUSSION

The nature of HLN, whether in human or animal bodies, remains unclear since Gibbes first described it in 1884 [1]. Previous studies have shown that HLN was defined as the brownish-red node macroscopically, and the nodular sinuses were filled with an abundance of erythrocytes microscopically [2-12]. Studies have always been limited to the anatomical field. In addition, the existence and nature of HLN in the human body remain controversial. Until recently, it has been reported that HLN model of the rat could be established by transferring the allogenic renal tissue [14]. Furthermore, it was also pointed out that MEL and ML rosettes were the key cellular complex for an immune response. Therefore, the HLN was considered as an immunomorphological organ.

However, compared to the animal experiment, results from this study have shown that: 1) Four types of HLN (Fig. 2), where results were well matched, based on the daily development process of HLN in the previous rat study [14]. 2) Binuclear macrophages (promonocytes), adhered by erythrocytes around, were found in the dilated sinuses of the node (Figs. 3C, 4A, and 4B rows) [15, 16]. Generally, the macrophage was a kind of mature cell in monocytes line. To date, no reports of macrophages undergoing selfdivision or proliferation in lymph nodes have been observed [17]. 3) Bi-, tri-, and tetranuclear lymphocytes (dividing lymphoblasts) (Figs. 4A and 4B rows) were also found gathering in dilated sinuses of the node, which was usually described to be found in the follicle and paracortical regions [18]. Combining these findings together for analysis (Figs. 4D and 4E rows), we assume that they were the static histopathological manifestations of the dynamic regeneration process of the degenerated lymph node (Note: the node with the dilated sinuses is a type of degenerated node) (Fig. 5) [14, 19, 20]. This process could promote the enhancement of the human immune system. Therefore, from an immunological perspective, the process of HLN manifestation changes was the proliferation and evolution of various immune cells in lymph nodes, especially in dilated sinuses, after being stimulated by antigens [18, 19]. Based on this study, the antigen could be considered cancer cells (endogenous antigen). On the basis of this assumption, some further studies including the molecular biology on the mechanisms of its occurrence and development will undoubtedly be beneficial for clinical diagnosis and treatment of related diseases.

In addition, the presence of CD68(+) cells (macrophages) within and around the metastatic tumor tissue (Figs. 4D and 4E rows) suggested that macrophages might attempt to kill cancer cells and prevent cancer cells from spreading [21]. As shown in Figure 4E, two metastatic nodes were harvested from the same group. Both were stained with CD68; one node on the right had a large number of CD68(+) cells (macrophages) within and around the metastatic tumor, as well as in sinuses of the residual lymphoid tissue, compared to the node on the left side. Furthermore, cellular structures were not observed within the tumor of the right node (Fig. 4E right image), which were eliminated by macrophages or their secretion [22]. Additionally, it is necessary to determine if these macrophages represent different subtypes or the same type of cells as those observed in HLN stimulated by allogeneic renal tissue translation or Escherichia coli injection in rat studies [14].

Studies on human HLN, especially on the relationship between HLN and cancer cases, are limited [4]. Table 1 and Figure 1 show that peritumoral HLN can occur in both non-metastatic and metastatic nodes in each case. Therefore, further studies should be conducted to understand the mechanisms of its occurrence and development in HLN of cancer patients.

CONCLUSION

Four histopathological types of the hematolymph nodes (HLN) were identified in specimens from 20 patients with gastrointestinal or breast cancer, where proliferating macrophages and lymphocytes were observed. In two of them, a large number of CD68(+) cells were observed around and within the metastatic tumors, while no cellular structure could be seen within tumor cells themselves. These histopathological types and cytological changes in HLN are considered to be static manifestations of the dynamic regeneration process of degenerated lymph nodes in tumor immunity.

Author contributions

WRP conceptualized and designed the study, performed the experiment, analyzed data, and wrote the

manuscript; FZ and YNZ performed histological sections, HE, and IHC stainings; ZAL took part in the data analysis and manuscript preparation; CXM partially participated in the experiment and data collection; YL performed histological sections, IHC staining, and CLSM examination; and FQZ performed sample preparation and data collections. All authors have approved the manuscript for submission.

Funding This study supported by the National Natural Science Foundation of China (No.
31671253); Xuzhou Medical University President Special Fund (No. 53051116); Xuzhou
Medical University Foreign Experts Special Fund, Department of International Cooperation and Exchange, Xuzhou Medical University (No. 537101).

Data Availability Statement This manuscript does not report data generation or analysis.

Acknowledgments
Many thanks to Dr. Fuxing Dong for his enthusiastic help during the experiment of laser scanning confocal microscopy in the Public Experimental Research Center, Xuzhou
Medical University.

Declarations
Ethical approval and consent to participate This study was performed with appropriate institutional ethics approval (approval no.: KY2022-110-01) in accordance with the principles of the Declaration of Helsinki. Informed consent was obtained via an opt-out method.

Competing interests Authors declare no potential conflicts of interest.

REFERENCES

1. Gibbes H. On some structures found in the connective tissues between the renal artery and vein of the human subject. Quart J Micr Sc 1884; 24:186-90.
2. Robertson WF. The prevertebral haemolymph glands. Lancet 1890; 136(3509): 1152–4.
3. Warthin AS. Normal histology of the human hemolymph glands. Am J Anat 1901; 1:63-80.
4. Jordan HE. Hemal nodes in Man. Anat Rec 1934; 59(8):297-310.
5. Nopajaroonsri C, Luk SC, Simon GT. The structure of the hemolymph node - a light, transmission, and scanning electron microscopic study. J Ultrastr Res 1974; 48:325-41.
6. Kazeem AA, Reid O, Scothorne RJ. Studies on hemolymph nodes. I. Histology of the renal hemolymph node of the rat. J Anat 1982; 134(4): 677-83.
7. Kazeem AA, Scothorne RJ. Studies on hemolymph nodes II. The regional origin of the afferent lymphatics. J Anat 1982; 135(1):1-4.
8. Hogg CM, Reid O, Scothorne RJ. Studies on hemolymph nodes III. Renal lymph as a major source of erythrocytes in the renal hemolymph node of rats. J Anat 1982; 135(2):291-9.
9. Zidan M, Pabst R. Histological, histochemical and immunohistochemical study of the haemal nodes of the dromedary camel. Anat Histol Embryol 2004; 33(5):284-9.
10. Pototska OYu, Lapsar HS. Subtypes of human atypical lymph nodes, defined based on comparative morphological analysis. Morphologia 2016; 10(2):45-52.
11. Akaydin Y, Kabak M. First description and morphology of haemal nodes in piglets (Sus scrofa domestica). Acta Vet Hung 2006; 54(2):135–42.
12. Zidan M, Pabst R. Histology of hemal nodes of the water buffalo (Bos bubalus). Cell Tissue Res 2010; 340(3):491-6.
13. Boqacz K, Slusarczyk K, Bibulek-Boqacz A. Attempt to identify hemolymph nodes in humans. Med Sci Monit 2000; 6(6):1082-4.
14. Pan WR, Liu Z, Sun DX, *et al.,* Hemolymph Node - An Immunomorphological Organ: Modeling the Hemolymph Node by Allografting Renal Tissue in the Rat. Cells Tissues Organs. 2023; 212(2):147-154. Epub 2021 Oct 25.
15. Lindberg MR, Lamps LW. Diagnostic pathology, Normal histology, 2nd Ed., 2017, Elsevier, Philadelphia, PA, USA.
16. Ovchinnikov DA. Macrophages in the embryo and beyond: much more than just giant phagocytes. Genesis. 2008; 46(9):447-62.
17. Gray EE, Cyster JG. Lymph node macrophages. Journal of Innate Immunity. 2012; 4 (5–6): 424–436.
18. Chaplin DD. Overview of the immune response. J Allergy Clin Immunol. 2010; 125(2 Suppl 2):S3-23.
19. Pan WR, Suami H, Taylor GI. Senile changes in human lymph nodes. Lymphatic Research & Biology, 2008; 6(2):77-83.
20. Pan WR, Liang S, Sun DX, *et al.,* Hemolymph Nodes Found In the Iliolumbar Region of a Tail Infected Rat. Sch Acad J Biosci, 2021 Oct 9(10): 290-292.
21. Galdiero MR, Garlanda C, Jaillon S, *et al.,*, Tumor associated macrophages and neutrophils in tumor progression. Journal of Cellular Physiology. 2013; 228 (7): 1404–1412.
22. Fu YL, Harrison RE. Microbial Phagocytic Receptors and Their Potential Involvement in Cytokine Induction in Macrophages. Frontiers in Immunology. 2021; 12: 662063.